



2301-9069 (e)
1829-8370 (p)

Kapal: Jurnal Ilmu Pengetahuan dan Teknologi Kelautan (Kapal: Journal of Marine Science and Technology)

journal homepage : <http://ejournal.undip.ac.id/index.php/kapal>



Integrity Assessment of Wall Distorted of Buried Gas Pipeline

Wira Herucakra¹⁾, Luh Putri Adnyani^{2) *)}, Lukytoardi Megantoro³⁾

¹⁾Universitas Indonesia (UI), Depok 16424, Indonesia

²⁾Institut Teknologi Kalimantan, Karang Joang, 76127Indonesia

³⁾PT. Dinamika Teknik Persada, Tangerang Selatan 15310, Indonesia

^{*)} Corresponding Author: luhputria@lecturer.itk.ac.id

Article Info

Abstract

Keywords:

Pipeline;
Buried; buckling;
Wall distorted;
Integrity assessment;
Finite element analysis

Article history:

Received: 10/08/2022
Last revised: 26/09/2022
Accepted: 01/11/2022
Available online: 01/11/2022
Published: 08/02/2023

DOI:

<https://doi.org/10.14710/kapal.v20i1.48231>

In the oil and gas industry, the pipeline is the main mode to transport the product and can be applied for long-distance transportation; hence some pipe segments may be buried underground. Buckling as the main cause of pipeline deformation and failure is often found at the in-service buried pipeline during inspection activity. Changes in laying conditions such as design and operational parameters, human activity and geological movement can affect the redistribution of deformation that may lead to pipe buckling. This paper presents a methodology that integrates inspection results and finite element analysis for the distorted wall of the pipeline. Inspection reported anomaly cases of wall distorted at buried gas pipeline, and the result will be used to do stress analysis using finite element analysis. Three different conditions within the different treatment of bedding conditions were assessed: pipe buried on uncompacted soil, pipe buried with rock bedding, and pipe buried in compacted soil. The result shows that the deteriorated pipe can be considered acceptable when buried in compacted soil. This condition may be used for further action and consideration, such as a mitigation strategy to maintain the safety and integrity of the deteriorated pipe.

Copyright © 2023 KAPAL : Jurnal Ilmu Pengetahuan dan Teknologi Kelautan. This is an open-access article under the CC BY-SA license (<https://creativecommons.org/licenses/by-sa/4.0/>).

1. Introduction

In the oil and gas industry, the pipeline is the main mode to transport the product. The pipeline can be applied for long-distance transportation; hence some sections of pipe segments may be buried underground. Loads are exerted on buried pipes by the soil that surrounds them. Besides the soil pressure, another load that may be subjected to the buried pipeline during the construction to their in-service phase are longitudinal loading (i.e. ununiform bedding support, differential settlement and ground movement; wheel load or live load (i.e. highway and railroad, aircraft load); soil subsidence; temperature; seismic; frost load, expansive soil and flotation (i.e. soil wedge, liquefaction, soil bearing and internal vacuum) [1].

Pipeline integrity is the cornerstone of many industrial and engineering systems. Kishawy and Gabbar [2] provides a review and analysis of all aspects related to pipeline integrity. While, Adumene, et al. [3] investigated pipeline integrity assessment regarding steel structural failure behavior considering the material and parametric uncertainties. The synergistic effects of hydrogen on the integrity assessment of a pre-cracked steel pipeline were analysed by Bouledroua, et al. [4]. Furthermore, Karamanos [5] reported an overview of the mechanical behaviour of steel pipes (elbows), which are critical components for the structural integrity of piping systems and pipelines, based on previously reported analytical solutions, numerical results, and experimental data.

In general, buckling is the main cause of pipeline deformation, and failure may lead to oil and gas leakage, fire and explosion to facility shut down. It will bring huge losses in the business (loss of product and facility), environmental impact (pollution), safety (injury to fatality) and company reputation [6]. In addition, accidental loads such as landslides may cause the failure of the buried pipeline [7] or pipeline subjected to reverse fault movement [8, 9].

Pipeline periodic inspection is required to be performed by the operator to ensure the integrity of the system and also part of compliance with government regulation. It can be performed by non-destructive testing to investigate the presence of anomalies in the pipe body. This inspection is conducted on the existing buried pipeline to investigate

the pipeline condition due to aging (i.e., corrosion). The realistic pipe stress needs to be calculated to ensure safety across the entire lifetime [10, 11]. Inspection of the buried pipeline is conducted by digging the buried pipeline and then tested the unburied pipeline. After the inspection, the stress analysis of the buried steel pipeline needs to be analysed. There are existing analytical methods for this stress analysis, for example, at crossings with active strike-slip faults [12] or the use of probability theory to assess the accuracy of the reconstructed position of a pipeline and obtained stress values [13]. Software to analyse stress analysis is also developed rapidly with the development of technology [14-16]. An in-service inspection is required to be performed periodically, commonly every four years, to ensure the integrity of the pipeline system and part of compliance in order to continue operating based on applicable government regulations. Through pipeline in-service inspection, the presence of anomaly can be detected, investigated, and assessed further. There are several inspection methods usually performed for the in-service pipeline, as summarised in Table 1.

This paper will assess and discuss anomaly cases found during pipeline in-service inspection activity. A buried section of the gas pipeline was measured, and an anomaly was found as the wall distorted along 233 cm located with pipe orientation of 4 o/c to 6.30 o/c with the maximum buckle of 7.60-mm inside and 0.70 mm outside the pipe body. Figure 1 shows detailed damage mapping activity performed on the suspected pipe segment.

Table 1. Rigid Pipeline Inspection Method [17-23].

Location	Section	Method
Onshore pipeline	Aboveground	<ul style="list-style-type: none"> ▪ Right of Way (ROW) Survey/pipeline patrol ▪ In-line inspection (ILI) / intelligent pigging ▪ Ultrasonic thickness (UT) spot ▪ Visual inspection (coating/ painting, corrosion, safety device)
	Underground	<ul style="list-style-type: none"> ▪ ROW Survey/pipeline patrol ▪ ILI / intelligent pigging ▪ UT spot ▪ Bell hole inspection (coating/wrapping, corrosion) ▪ CIPS (Close interval potential survey) / DCVG (Direct current voltage gradient) ▪ Cathodic Protection (CP) potential measurement (CuCuSO₄) ▪ Soil Resistivity & Soil pH measurement (soil corrosivity)
Offshore pipeline	Riser Section	<ul style="list-style-type: none"> ▪ Remote Operated Vehicle (ROV) / Subsea / underwater Inspection (for submerged and splash zone) ▪ ILI / intelligent pigging (for all sections of the riser) ▪ UT spot (for topside and atmospheric zone) ▪ Visual inspection (coating/painting, corrosion, safety device)
	Subsea Pipeline	<ul style="list-style-type: none"> ▪ CP potential measurement (AgAgCl) ▪ ROV / SSS / Subsea / underwater inspection ▪ Subsea CP inspection ▪ ILI / intelligent pigging

As the anomaly is confirmed, an immediate assessment is required to understand potential hazards that may arise produced by the current wall distorted anomaly. Pipe buckling includes local buckling (pipe wall buckling) and overall buckling. Local buckling is mainly caused by external pressure or internal pressure, axial force and bending moment. In the case of only external pressure, pipeline collapse is likely to occur [6].



Figure 1. Detailed damage mapping from direct measurement.

2. Methods

Figure 2 present flow process of integrity assessment of wall distorted buried gas pipeline consist of two main phases, they are: solution validation of normal pipe condition and continued to integrity assessment of deteriorated pipe condition. In the solution validation of normal pipe condition phase, the solution of FEM model for normal pipe condition in term of effective stress will be validated against empirical solution based on API 1102. The API 1102 provides step by step calculation of empirical solution in term of effective stress of buried pipeline that is inline with the formulation of shell element used to develop FEM model. The detailed empirical solution calculation based on API 1102 is discussed in the section 2.3. The solution of FEM model of normal pipe condition is shall satisfy compared to the empirical solution with the error limited to 5%. Based on the satisfying FEM model of normal pipe condition then continued to develop FEM model for deteriorated pipe condition based on inspection data as discussed in the section 2.2. the simulation will be performed under different condition to understand the effect on the different treatment of burial condition of the deteriorated pipe.

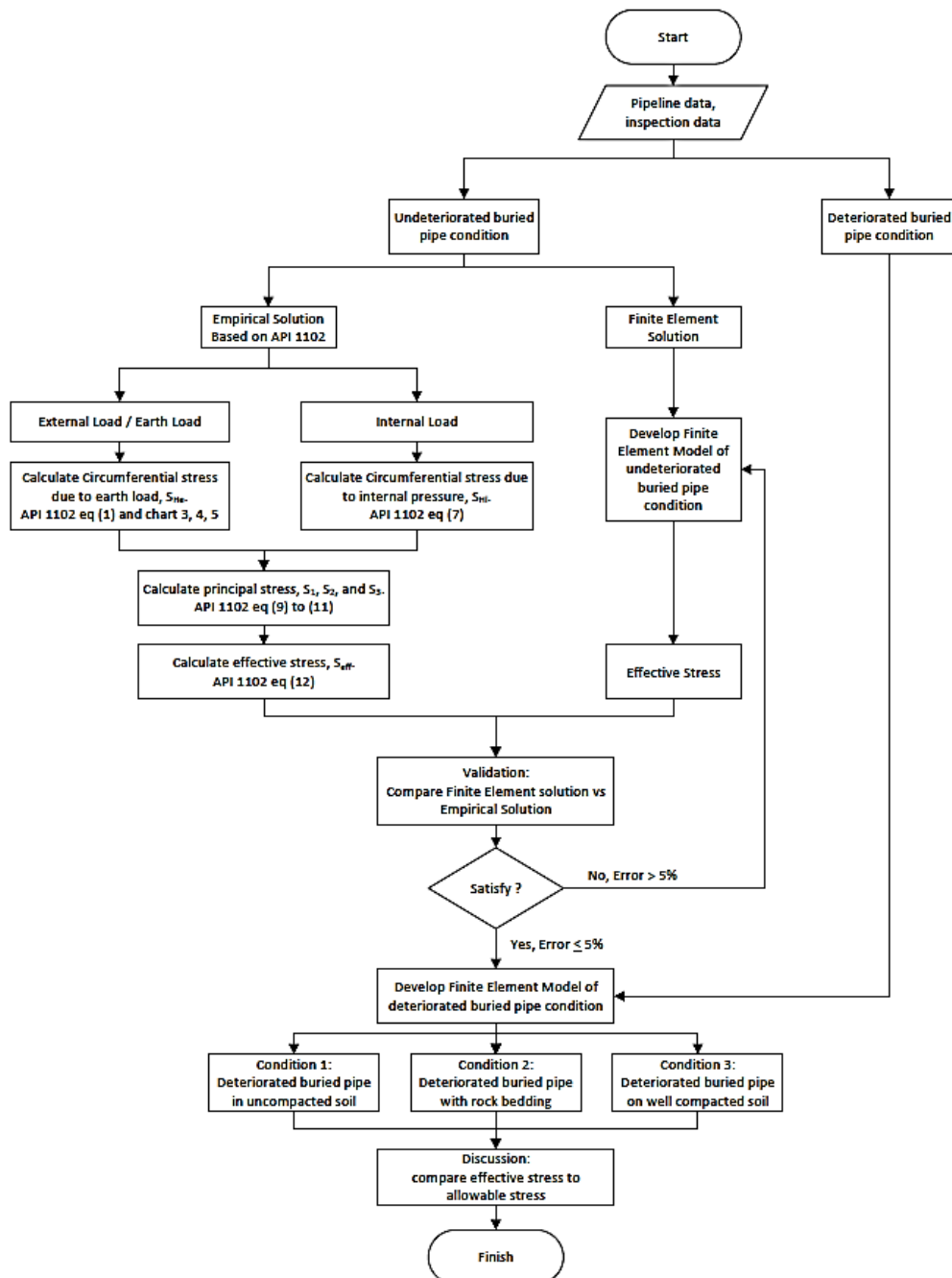


Figure 2. Flow process of integrity assessment of wall distorted of buried gas pipeline.

2.1. Pipeline Data

The general data of the pipeline to be analysed is presented in Table 2. Pipeline and site properties data in Tables 2-4 will be used to model the pipeline in software for finite element analysis.

Table 2. Pipe and characteristic operational data

Parameter	Value
Diameter, D	28-inch
Length	30 km
Wall thickness, t_w	8.7 mm (0.342 inch)
Steel grade	API 5L X65
Specified minimum yield stress, $SMYS$	65000 psi
Pipe type	Spiral / longitudinal weld
MAOP, P	1060 psig
Design pressure	1150 psig
Design factor, F	0.72
Longitudinal joint factor, E	1
Installation temperature, $T1$	80 °F
Max or min operating temperature, $T2$	100° F
Temperature derating factor, T	1
Year commissioning	2003
Pipe product	gas

Table 3. Steel properties and characteristic operational data

Parameter	Value
Young modulus, E_s	$2.9 \cdot 10^7$ psi
Poisson ration, ν_s	0.3
Coefficient of thermal expansion, αT	$6.5 \cdot 10^{-6}$ in/F

Table 4. Installation and site characteristic data

Parameter	Value
Depth, H	5.9 ft
Soil boring diameter, Bd	28 inches
Soil type	A
Modulus of soil reaction, E'	0.5 Ksi (*)
Resilient modulus, E_r	10 ksi (**)
Unit weight, γ	120 lb/ft ³
Type of longitudinal weld	Seamless
Design of wheel load from a single axis, P_s	N/A
Design of wheel load form tandem axis, P_t	N/A
Pavement type	N/A

Note:

*) based on API 1102 Table A.1 – Typical value for modulus of soil reaction, E'

**) based on API 1102 Table A.2. – Typical value for resilient modulus, E_r

2.2. Inspection Data

UT test is conducted in the buried pipeline, but no decrement in thickness. However, visually, the pipeline is dented or wrinkled in a different area of the pipeline's section. Then, a direct measurement test is tested in the pipeline. Anomalies findings are a wall distorted along of 1079 mm located pipe orientation of 4 o/c to 6.30 o/c with the maximum buckle of 7.60-mm inside and 0.70 mm outside the pipe body..

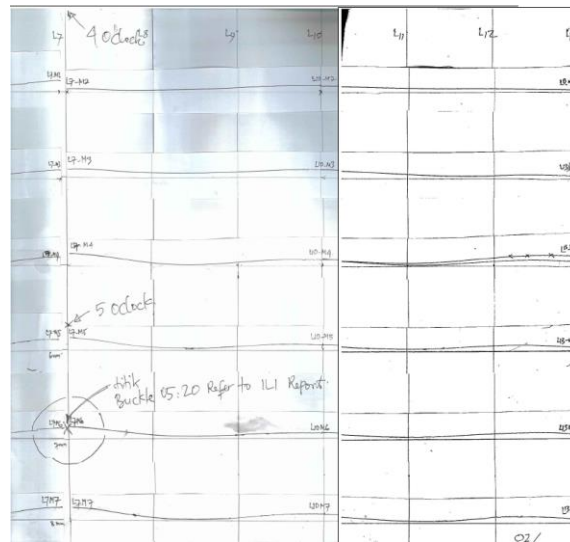


Figure 3. Example of the contour of the distorted wall from inspection record

Shell buckling (or wall distortion) tends to occur when the diameter-thickness ratio of the pipeline is greater than 26 [24]. Changes in the laying condition of the buried pipeline, such as design and operational parameters, human activity and geological movement, can affect the redistribution of deformation and lead to pipe buckling. Figure 3 show inspection record data collected by the pipeline inspector, and Figure 4 present the numerical data of distorted wall in term of the adjusted pipe radius.

		Longitudinal (1079 mm)												
		1	2	3	4	5	6	7	8	9	10	11	12	13
Transverse (4 o/c to 6.30 o/c)	1	355.6	355.6	355.6	355.6	355.6	355.6	355.6	355.6	355.6	355.6	355.6	355.6	355.6
	2	355.6	355.6	357.8	357.2	357.9	358.9	362.7	356.9	358.1	359.4	358.1	358.1	357.2
	3	357.0	354.9	356.5	359.0	357.5	357.5	360.4	358.5	358.9	360.4	358.1	357.3	357.1
	4	356.3	355.6	356.5	358.3	356.1	356.4	362.3	358.0	357.9	359.1	356.4	358.4	358.6
	5	356.2	356.0	357.2	358.9	356.8	358.8	363.0	357.3	357.8	359.0	357.1	359.0	357.7
	6	356.5	356.6	357.2	359.0	359.6	357.2	362.9	358.0	357.8	358.9	357.1	358.8	358.7
	7	357.3	356.5	356.5	359.2	356.7	358.4	363.2	357.2	357.4	359.8	356.8	359.3	358.1
	8	358.3	357.5	356.4	359.5	357.0	357.6	361.3	357.5	356.3	358.5	357.6	357.1	359.2
	9	359.1	355.6	357.0	357.8	356.6	356.6	358.7	356.8	356.1	358.7	356.9	357.7	356.9
	10	357.5	357.8	356.3	357.5	356.8	356.3	357.4	357.1	355.6	357.4	356.7	358.0	359.6
	11	361.0	357.9	357.3	355.6	356.1	358.6	361.7	359.6	356.0	357.0	355.6	358.2	360.0

Figure 4. Numerical data of distorted wall (in terms of adjusted pipe radius).

2.3. Pipe Stress Calculation of Un-Deteriorated Buried Pipe Based on API 1102

The recommended practice of API RP 1102 [25] provides step by step calculation of empirical solution in term of effective stress of buried pipeline that is in line with the formulation of shell element used to develop FEM model. This calculation is performed to validate the effective stress produced from finite element analysis considering buried undeteriorated pipe conditions as described in the flow process (see Figure 2). The section of deteriorated pipe that will be analysed using finite element is buried underground without any presence of rail and/or road crossing at the surface and also neglect the effect of thermal expansion. Hence, the live load due to rail and/or road crossing is neglected since the stress calculation is based on API 1102. It may affect the calculation of cyclic circumferential stress due to live load, and the cyclic longitudinal stress due to live load will be eliminated during the calculation of principal stresses.

2.3.1. Internal Load

The circumferential stress due to internal pressure, S_{Hi} is calculated based on API 1102 section 4.7.3, affected by internal pressure, diameter and wall thickness as follows.

$$S_{Hi} = p \frac{(D - t_w)}{2t_w} \tag{1}$$

Based on Equation 1 and following flowchart in Figure 2, circumferential stress due to internal pressure, S_{Hi} , is 42,862 psi.

2.3.2. External Load

The internal load is calculated based on API 1102 section 4.7.2.1, the circumferential stress at the pipeline invert caused by earth load, S_{He} , that has a linear relation with soil properties, diameter and also soil properties is determined as:

$$S_{He} = K_{He} B_e E_e \gamma D \tag{2}$$

Based on Equation 2 and following flowchart in Figure 2, circumferential stress at the pipeline invert caused by earth load, S_{He} is 5,817.78 psi. While the stiffness factor for circumferential stress from earth load, K_{He} , the burial factor for earth loading, B_e , and the excavation factor for earth load, E_e , is taken from the API 1102 Figures 5-7.

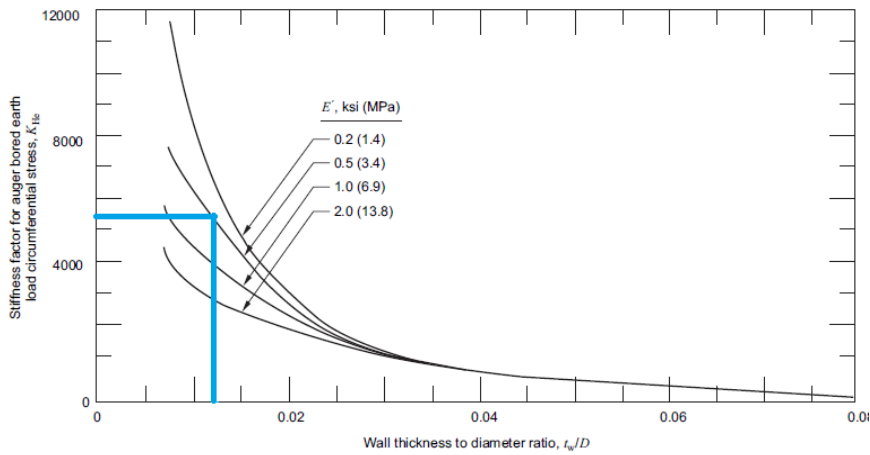


Figure 5. Stiffness factor of earth load circumferential stress, K_{He} , $t_w/D = 0.012$ and $E' = 0.5$ ksi. (Adopted from API 1102)

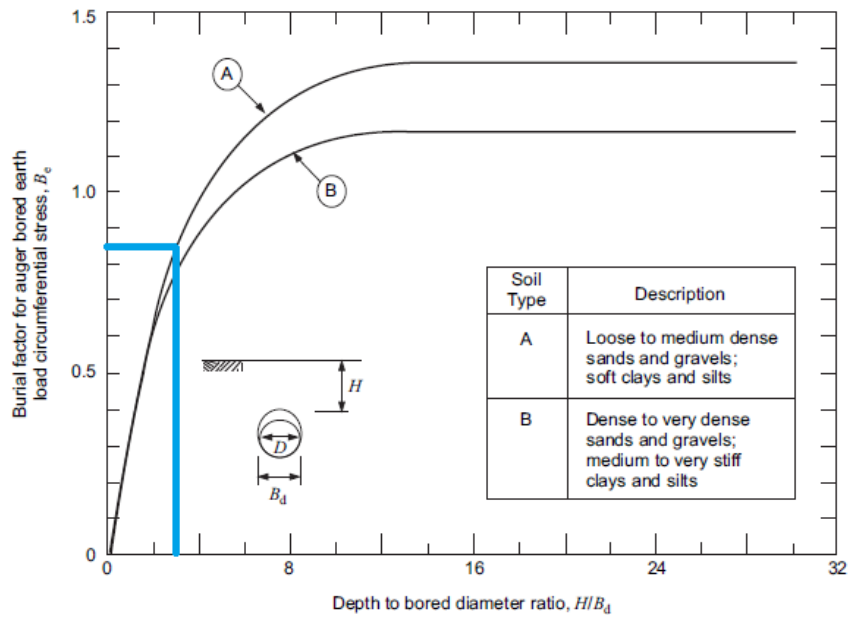


Figure 6. Burial factor for earth load circumferential stress, B_e , $H/B_d = 2.53$, soil type A and $B_e = 0.85$. (Adopted from API 1102)

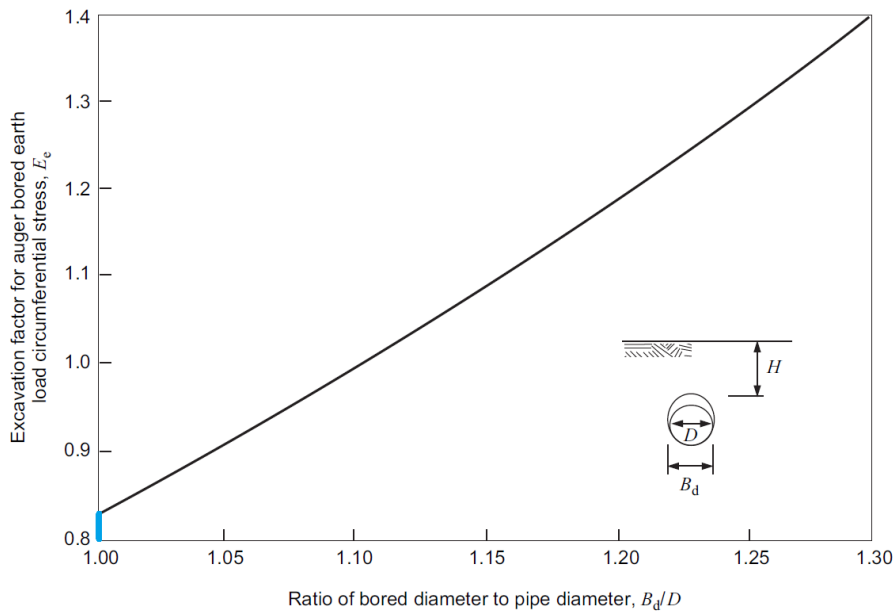


Figure 7. Excavation factor for earth load circumferential stress, E_e , $B_d/D = 1.0$ and $E_e = 0.80$. (Adopted from API 1102)

2.3.3. Principal Stress

The principal stress of the maximum circumferential stress, S_1 , the maximum longitudinal stress, S_2 and the maximum radial stress, S_3 is calculated based on API 1102 section 4.8.1.2 as follows:

$$S_1 = S_{He} + S_{Hi} \tag{3}$$

$$S_1 = 48680.00 \text{ psi}$$

$$S_2 = v(S_{He} + S_{Hi}) \tag{4}$$

$$S_2 = 14603.88 \text{ psi}$$

$$S_3 = -p = -MAOP \tag{5}$$

Based on Equation 5 and following flowchart in Figure 2, maximum radial stress that depend on maximum circumferential stress (S_1) and maximum longitudinal stress (S_2), S_3 , is -1,060.00 psi.

2.3.4. Effective Stress

The total effective stress, S_{eff} is calculated based on API 1102 section 4.8.1.3, as follows:

$$S_{eff} = \sqrt{\frac{1}{2}[(S_1 - S_2)^2 + (S_2 - S_3)^2 + (S_3 - S_1)^2]} \tag{6}$$

Based on Equation 6 and following flowchart in Figure 2, total effective stress, S_{eff} is 44,048.49 psi.

2.4. Finite Element Analysis of Wall Distorted Pipeline

According to the geometrical characteristics of pipe structure, the research method of pipe buckling failure can be regarded as a cylindrical shell structure. Scholars have done a lot of research on the local buckling of cylindrical shells [6, 26]. The finite element analysis of wall distorted pipeline will be aided by STAAD Pro commercial software. The elastic stress analysis will be performed by utilising STAAD Pro element library of the plate/shell element based on hybrid element formulation. The element can be 3-nodded (triangular) or 4-nodded (quadrilateral) with six degrees of freedom per node. The thickness of the element can be assigned different from one to another.

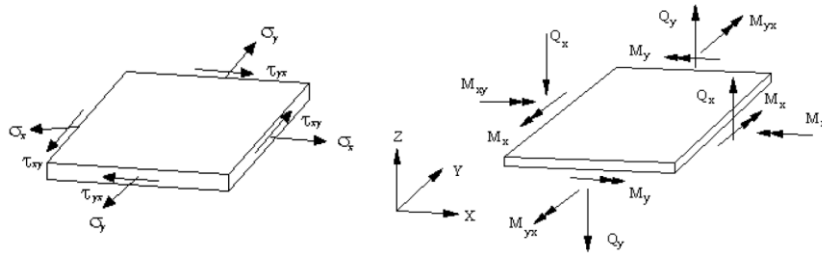


Figure 8. Quadratic stress distribution of STAAD Pro plate/shell hybrid element formulation – plane stress action (left) and bending action (right). (Adopted from STAAD Pro Technical Reference Manual) [27].

The out-of-plane rotational stiffness from the plane stress portion of each element is useful incorporated and not treated as a dummy. Despite incorporating the rotational stiffness, the element absolutely satisfies the patch test. The out-of-plane shear strain energy is incorporated in the formulation of the plate bending component. As a result, the element responds to Poisson boundary conditions which are considered to be more accurate than the customary Kirchhoff boundary condition. The plate bending portion can handle thick and thin plates, thus extending the usefulness of the plate element to a multiplicity of problems. In addition, the thickness of the plate is taken into consideration in calculating the out-of-plane shear. The equivalent stress equation of shell element expressed as Equation 7:

$$S = \sigma_e = \frac{1}{\sqrt{2}} \sqrt{(\sigma_{max} - \sigma_{min})^2 + \sigma_{max}^2 + \sigma_{min}^2} \tag{7}$$

where

$$\sigma_{max} = \frac{(\sigma_x + \sigma_y)}{2} + T_{max} \tag{8}$$

$$\sigma_{min} = \frac{(\sigma_x + \sigma_y)}{2} - T_{max} \tag{9}$$

$$T_{max} = \sqrt{\frac{(\sigma_x - \sigma_y)^2}{4} + \tau_{xy}^2} \tag{10}$$

$$\sigma_x = S_x + \frac{M_x}{Z} \tag{11}$$

$$\sigma_y = S_y + \frac{M_y}{Z} \tag{12}$$

$$\tau_{xy} = S_{xy} + \frac{M_{xy}}{Z} \tag{13}$$

Where the S_x , S_y and S_{xy} are membrane stress, M_x , M_y , and M_{xy} are bending moment, and the Z is the plastic sectional modulus.

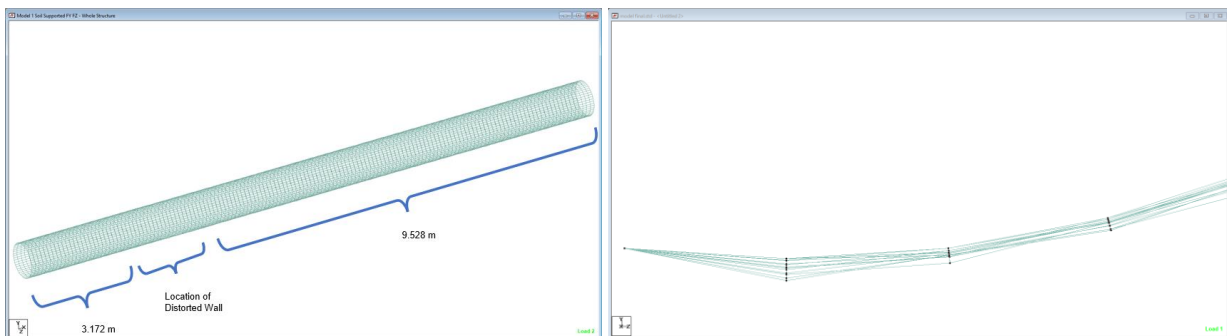


Figure 9. Isometric view (left); Cross section view (right)

A total of 7750 shell elements were used to build one section pipeline model with a total length of about 13.8 m, including deteriorated sections. The location of the distorted wall is about 3.172 m from the edge of the pipe. As

discussed in the previous section, the distorted wall model was taken from inspection data (see section 3). The preview of the model is presented in Figures 9 and 10.

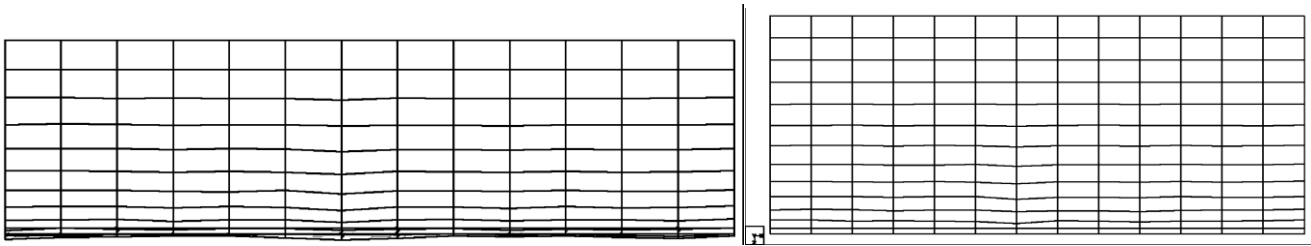


Figure 10. Side view (left); bottom view (right)

2.4.1. Boundary Condition

The boundary condition is set as pinned at both ends of the pipe. For undeteriorated buried pipe conditions, the soil support is applied as fixed in translation FZ and FZ and released for all moments as presented in the following Figure 11.

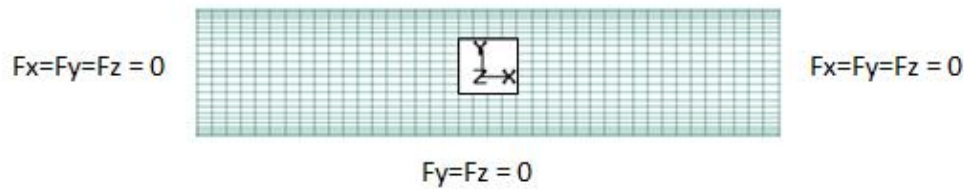


Figure 11. Boundary condition for undeteriorated buried pipe model.

2.4.2. Loading

Loading considered in the analysis consists of internal pressure load and external load (earth load). The internal pressure load applied on the pipe wall is MAOP as 1060 psi (0.75 kg/mm²), and the external load (earth load) applied for 1.8 m depth of soil is 0.00347 kg/mm². The preview of the applied load is presented in Figures 12 and 13.

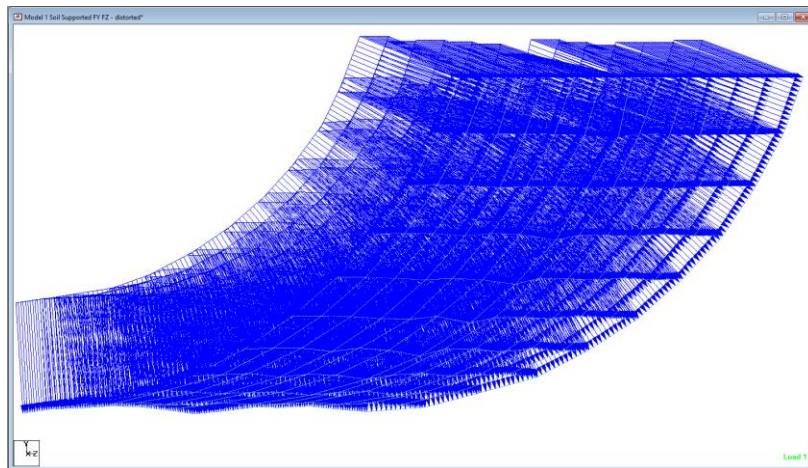


Figure 12. Internal pressure load, MAOP.

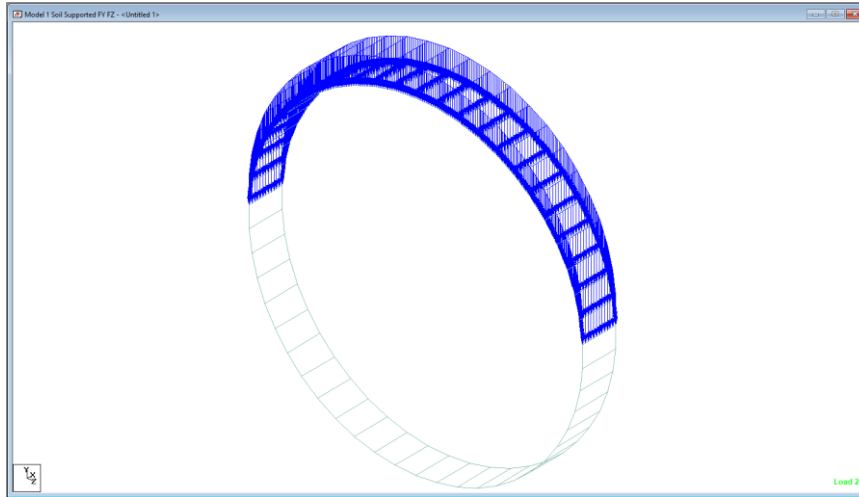


Figure 13. External load (earth load).

2.4.3. Validation

Validation was performed by comparing the result of the finite element analysis of undeteriorated pipe against stress calculation based on API 1102. The effective stress produced by finite element analysis of the undeteriorated pipeline, as presented in the Figure 14, is $42.5 \cdot 10^3$ psi, and the effective stress calculated based on API 1102 as discussed in the previous section, is $44.05 \cdot 10^3$ psi. The difference between both results is 3.5%. Hence it is considered acceptable since the difference is below 5%.

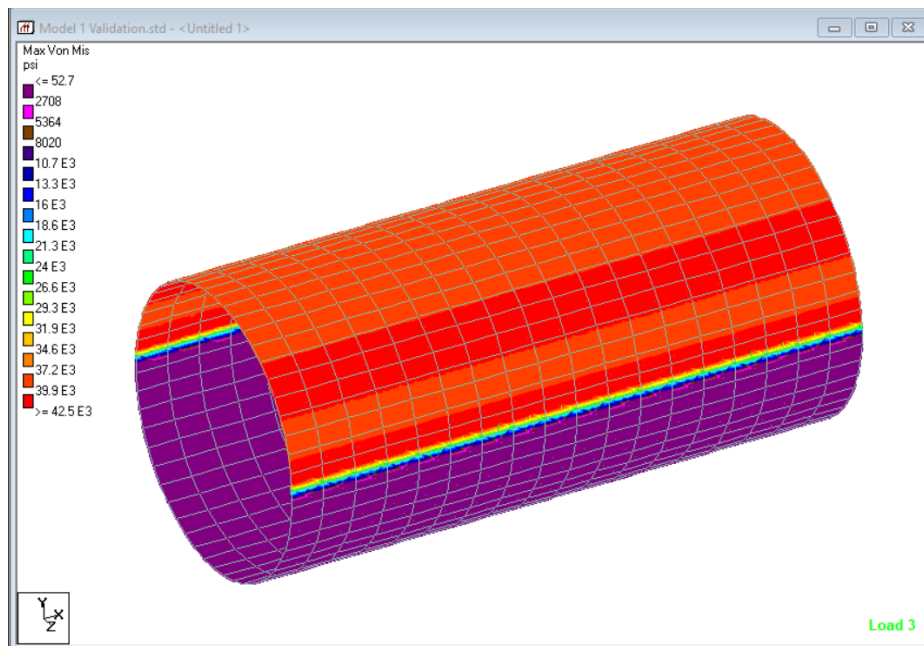


Figure 14. Effective stress of undeteriorated buried pipeline

3. Results and Discussion

Stress analysis of distorted wall pipe using finite element method was performed to understand the effect on the different treatment of burial condition of the deteriorated pipe. There are three conditions simulated in the analysis. Condition 1: Deteriorated pipe buried on uncompacted soil. This condition assumes the soil layer below the pipeline is un-compacted and has potentially collapsed. The boundary condition will be applied as pinned at both ends of the pipe, as shown in Figure 15. Condition 2: Deteriorated pipe buried with rock bedding. This condition assumes the pipe lay on rock bedding which provides restraint on the vertical displacement of the pipe but does not restrain in lateral and axial. The boundary condition will be applied as pinned at both ends of the pipe and fixed translation in the vertical direction (y-axis), as shown in Figure 16. Condition 3: Deteriorated pipe buried in compacted soil. This condition assumes soil treatment has been performed to make the soil around the pipe have the capacity to restrain vertical and lateral displacement. The boundary condition will be applied as pinned at both ends of the pipe and fixed translation in the vertical and lateral direction (y and z axis), as shown in Figure 17.

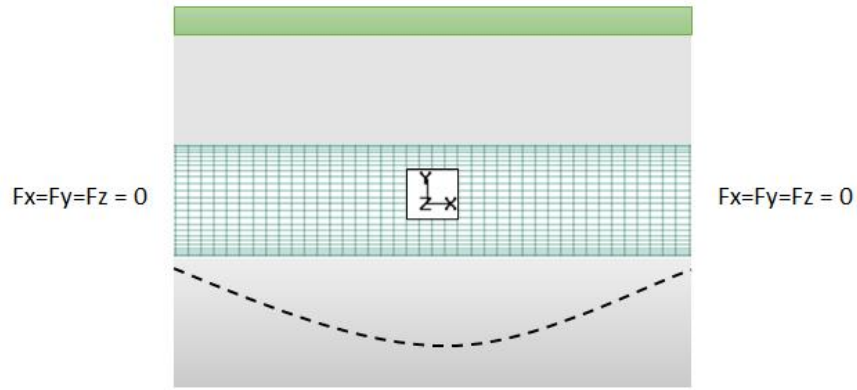


Figure 15. Condition 1: Deteriorated pipe buried in uncompacted soil

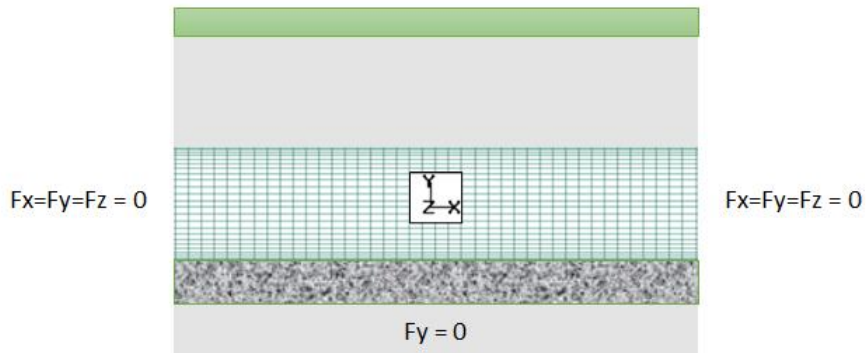


Figure 16. Condition 2: Deteriorated pipe buried with rock bedding

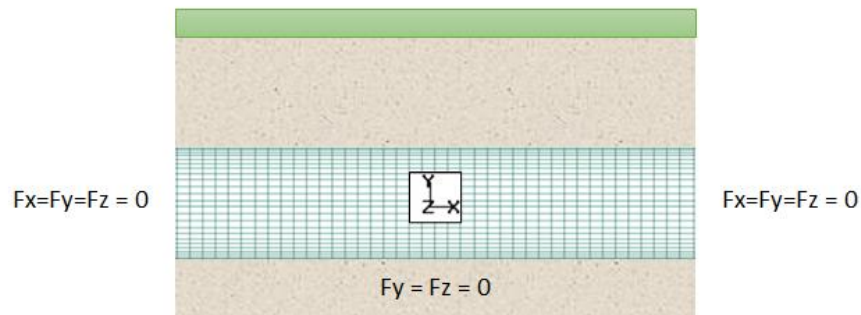
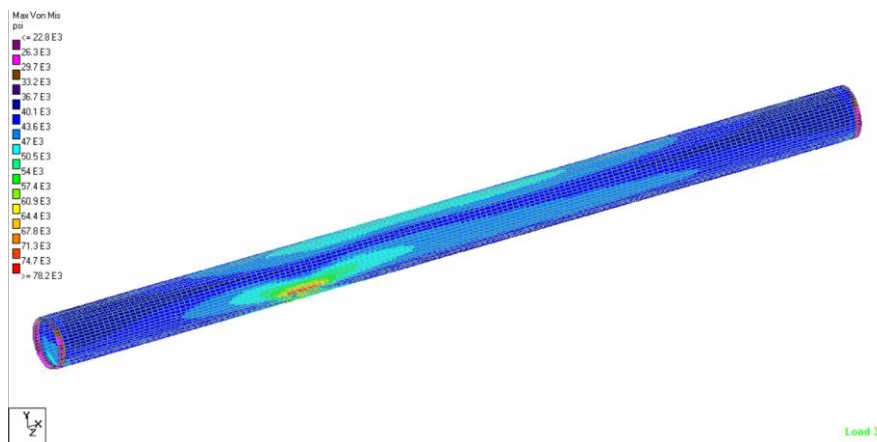


Figure 17. Condition 3: Deteriorated pipe buried on well-compacted soil



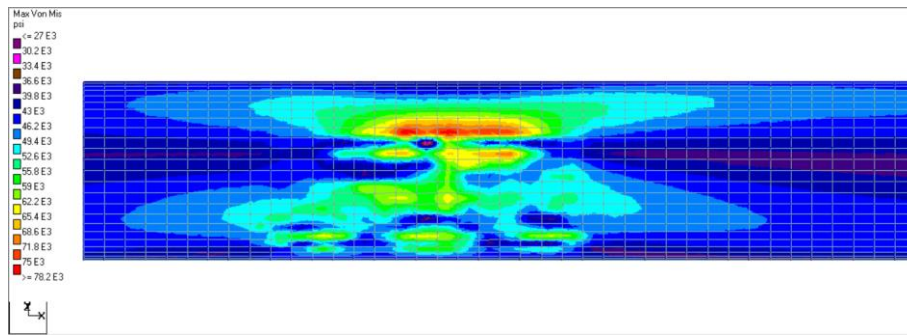


Figure 18. Max von mises stress for condition 1; isometric view (top), detailed view (bottom)

Condition 2

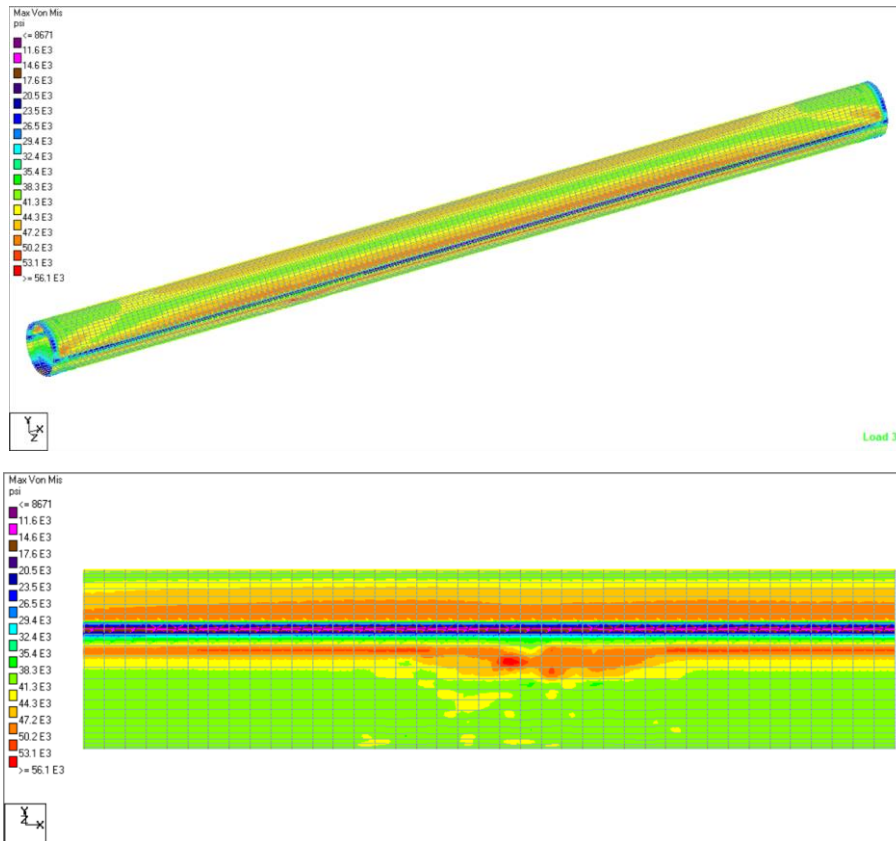
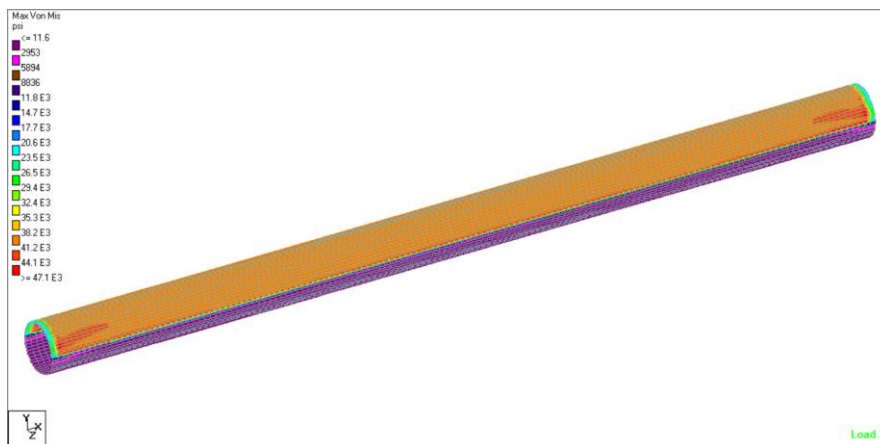


Figure 19. Max von mises stress for condition 2; isometric view (top), detailed view (bottom)

Condition 3



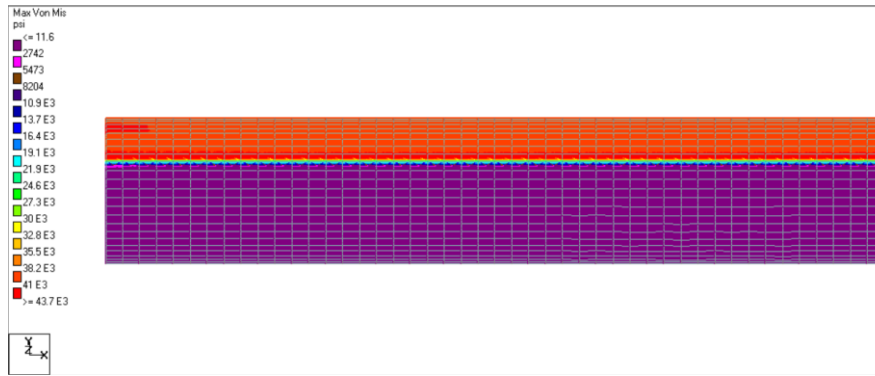


Figure 20. Max von misses stress for condition 3.

Figures 18 - 20 present the maximum von misses stress plot as a result of the analysis for different pipe laying treatment. The result of the analysis is summarized in Table 5 below. It is shown that different laying treatment of the buried pipeline has a significant effect, especially for the deteriorated pipe.

Table 5. Result summary

Condition	Effective stress	Allowable Stress	Remark
1 Deteriorated, hanging	78200 psi		Overstressed
2 Deteriorated, vertically supported	56100 psi	46800 psi	Overstressed
3 Deteriorated, vertical and laterally supported	43700 psi		Acceptable

Note:
 Allowable Stress = SMYS x F

A design factor of 0.72 for allowable stress is taken from API and ASME that will be used in this study. This allowable stress calculation used yield strength material as presented in Table 5. Based on the data, the hanging condition and vertically supported condition are not enough to maintain stress on the pipe. It is required careful pipe laying treatment such as soil compaction in order to restrain any vertical and lateral displacement of the buried pipeline. Compared to the design of new pipeline, allowable stress is related to internal pressure and wall thickness with safety factors 1.2 to 4.0 [28]. This safety factor is aligned with the recommendation by European and Japanese standards, which are 1.7 and 2.1, respectively [29]. In engineering practice, allowable stress related to material strength will be considered for the existing pipeline with wrinkle conditions and not in elastic conditions.

4. Conclusion

Based on the analysis that has been performed above, it can be concluded that: 1) as the inspection record, the maximum distortion at pipe wall was recorded as 7.60 mm buckle inside, and a minimum of 0.700 mm buckle outside of pipe body along 1079 mm pipe length and is located at pipe orientation of 4 o/c to 6.30 o/c; 2) the different pipe laying/bedding treatments produce different results of the effective stress; and 3) the deteriorated pipe can be considered acceptable when the laying/bedding treatment is performed carefully by soil compaction in order to restrict unwanted vertical and lateral displacement of the buried pipe. This acceptable conclusion is taken because effective stress is not exceeded than allowable stress.

Notations

- B_e The burial factor for earth load
- D Pipe outside diameter (in or mm)
- E Longitudinal joint factor
- E_e The excavation factor for earth load
- E_s Young modulus of steel (psi or kPa)
- F Design factor chosen in accordance with 49 Code of Federal Regulation Part 192.111 or part 195.106.
- K_{ia} The stiffness factor for circumferential stress form earth load
- p Internal pressure, taken as the MAOP or MOP (psi or kPa)
- S_{eff} Total effective stress (psi or kPa)
- S_{he} Circumferential stress at the pipeline invert caused by earth load (psi or kPa)
- S_{hi} Circumferential stress at the pipeline invert caused by internal pressure (psi or kPa)
- $SAYS$ Specified minimum yield strength (psi or kPa)
- S_1 The maximum circumferential stress (psi or kPa)
- S_2 The maximum longitudinal stress (psi or kPa)
- S_3 The maximum radial stress (psi or kPa)
- T Temperature derating factor

T_1	The temperature at time installation (°F or °C)
T_2	The maximum or minimum operating temperature (°F or °C)
t_w	Wall thickness (in or mm)
ν_s	Poisson's ratio of steel
α_T	The coefficient of thermal expansion of steel (per °F or per °C)
ΔS_H	Is ΔS_{He} for railroad or ΔS_{Hh} for highway (psi or kPa)
ΔS_L	Is ΔS_{Le} for railroad or ΔS_{Lh} for highway (psi or kPa)
γ	The soil unit weight (lb/in ³ or kN/m ³)

References

- [1] A. P. Moser and S. Folkman, *Buried pipe design*. McGraw-Hill Education, 2008.
- [2] H. A. Kishawy and H. A. Gabbar, "Review of pipeline integrity management practices," *International Journal of Pressure Vessels and Piping*, vol. 87, no. 7, pp. 373-380, 2010.
- [3] S. Adumene, F. Khan, S. Adedigba, S. Zendejboudi, and H. Shiri, "Offshore pipeline integrity assessment considering material and parametric uncertainty," *Journal of Pipeline Science and Engineering*, vol. 1, no. 3, pp. 265-276, 2021.
- [4] O. Bouledroua, Z. Hafsi, M. B. Djukic, and S. Elaoud, "The synergistic effects of hydrogen embrittlement and transient gas flow conditions on integrity assessment of a precracked steel pipeline," *International Journal of Hydrogen Energy*, vol. 45, no. 35, pp. 18010-18020, 2020.
- [5] S. A. Karamanos, "Mechanical Behavior of Steel Pipe Bends: An Overview," *Journal of Pressure Vessel Technology*, vol. 138, no. 4, 2016, doi: 10.1115/1.4031940.
- [6] H. Nie., W. Ma., X. He., X. Huo., Y. Wang., J. Ren., W. Dang., K. Wang., J. Cao., T. Yao., X. Liang., "Study on buckling deformation mechanism of pipeline crossing road," *Engineering Failure Analysis*, p. 106412, 2022.
- [7] L. Chen, S. Wu, H. Lu, K. Huang, Y. Lv, and J. Wu, "Stress analysis of buried gas pipeline traversing sliding mass," *The Open Civil Engineering Journal*, vol. 8, no. 1, 2014.
- [8] H. Hojat Jalali, F. R. Rofooei, and N. Khajeh Ahmad Attari, "Performance of Buried Gas Distribution Pipelines Subjected to Reverse Fault Movement," *Journal of Earthquake Engineering*, vol. 22, no. 6, pp. 1068-1091, 2017, doi: 10.1080/13632469.2016.1269694.
- [9] F. R. Rofooei, N. K. A. Attari, and H. Hojat Jalali, "New Method of Modeling the Behavior of Buried Steel Distribution Pipes Subjected to Reverse Faulting," *Journal of Pipeline Systems Engineering and Practice*, vol. 9, no. 1, 2018, doi: 10.1061/(asce)ps.1949-1204.0000296.
- [10] H. Hung, P. Rajeev, D. Robert, and J. Kodikara, "Stress analysis of buried pipes," in *Proceedings of the 8th Australasian Congress on Applied Mechanics 2014 (ACAM 8)*, 2014: Engineers Australia, pp. 510-518.
- [11] H. Liu, F. Khan, and P. Thodi, "Revised burst model for pipeline integrity assessment," *Engineering failure analysis*, vol. 80, pp. 24-38, 2017.
- [12] D. K. Karamitros, G. D. Bouckovalas, and G. P. Kouretzis, "Stress analysis of buried steel pipelines at strike-slip fault crossings," *Soil Dynamics and Earthquake Engineering*, vol. 27, no. 3, pp. 200-211, 2007.
- [13] I. V. Orynyak, I. V. Lokhman, and A. V. Bogdan, "Determination of curve characteristics by its discrete points measured with an error and its application to stress analysis for buried pipeline," *Strength of Materials*, vol. 44, no. 3, pp. 268-284, 2012.
- [14] B. Li, X. Li, Y. Miao, and H. Yang, "Application of Stress Analysis Software in Oil and Gas Pipeline," in *IOP Conference Series: Earth and Environmental Science*, 2020, vol. 558: IOP Publishing, p. 022006.
- [15] P. Vazouras, S. A. Karamanos, and P. Dakoulas, "Finite element analysis of buried steel pipelines under strike-slip fault displacements," *Soil Dynamics and Earthquake Engineering*, vol. 30, no. 11, pp. 1361-1376, 2010, doi: 10.1016/j.soildyn.2010.06.011.
- [16] X. Wu, Y. Jiang, H. Lu, S. Wu, and X. Chen, "Stress analysis of shallow sea gas pipelines," in *Pipelines 2013: Pipelines and Trenchless Construction and Renewals—A Global Perspective*, 2013, pp. 1444-1450.
- [17] *API Recommended Practice 1160 "Managing System Integrity for Hazardous Liquid Pipelines"*, API RP 1102, 2001.
- [18] *ASME B31. 4 Pipeline Transportation Systems for Liquid Hydrocarbons and Other Liquids*, ASME, 2009.
- [19] *ASME B31. 3 Process Piping*, ASME, New York, NY, USA, 2010.
- [20] *ASME B31.8S, "Managing System Integrity of Gas Pipelines"*, ASME, 2014.
- [21] *ASME B31.8 Gas Transmission and Distribution Piping Systems*, ASME, New York, 2016.
- [22] *Recommended Practice RP-F101 for Corroded Pipelines 2004*, DNV, Norway, 2004.
- [23] *Integrity Management of Submarine Pipeline System, Recommended Practice DNV-RP-F116*, Norway, 2009.
- [24] S. Kyriakides and G. T. Ju, "Bifurcation and localization instabilities in cylindrical shells under bending-I. Experiments," *International journal of solids and structures*, vol. 29, no. 9, pp. 1117-1142, 1992.
- [25] *API RP 1102, Steel Pipelines Crossing Railroads and Highways*. American Petroleum Institute, 2007.
- [26] Y. Yifei, S. Bing, W. Jianjun, and Y. Xiangzhen, "A study on stress of buried oil and gas pipeline crossing a fault based on thin shell FEM model," *Tunnelling and Underground Space Technology*, vol. 81, pp. 472-479, 2018.
- [27] *STAAD.Pro Technical Reference Manual*, i. Bentley Systems, 2013.
- [28] W. D. Callister and D. G. Rethwisch, *Materials science and engineering: an introduction*. Wiley New York, 2018.

- [29] L. Jeremić, B. Petrovski, B. Đorđević, and S. Sedmak, "Structural integrity assessment of welded pipeline designed with reduced safety," *Tehnički vjesnik*, vol. 27, no. 5, pp. 1461-1466, 2020.